LA-UR-12-20859
Approved for public release; distribution is unlimited.

Title:	Los Alamos National Laboratory W76 Pit Tube Lifetime Study
Author(s):	Abeln, Terri G.
Intended for:	Report

Weapon Systems Engineering Division		
Los Alamos National Laboratory W76 Pit Tube Lifetime Study		
Number: **W-9-TR-0143U** **LA-UR-XX-XXXX**	Revision **A**	Effective Date: **April 3, 2012**

Approved by	Name	Organization	Signature	Date
Authors:	Terri Abeln	W-9		3/29/2012
Group Leader	Charles Hills	W-9		4/03/2012

Status:	**Comments:**
☒ New ☐ Major Revision ☐ Minor Revision ☐ Reviewed, No Change	

This document has been deemed
UNCLASSIFIED by:

Charles Hills, W-9 CRH
(DC)

Los Alamos National Laboratory W76 Pit Tube Lifetime Study

Terri Abeln, W-9, Surveillance Oversight

Requested Investigation: A metallurgical study was requested as part of the Los Alamos National Laboratory (LANL) W76-1 life-extension program (LEP) involving a lifetime analysis of type 304 stainless steel pit tubes subject to repeat bending loads during assembly and disassembly operations at BWXT / Pantex. This initial test phase was completed during the calendar years of 2004-2006 and the report not issued until additional recommended tests could be performed. These tests have not been funded to this date and therefore this report is considered final.

Summary: Tubes were reportedly fabricated according to Rocky Flats specification P14548 – *Seamless Type 304 VIM/VAR Stainless Steel Tubing*. Tube diameter was specified as 0.125 inches and wall thickness as 0.028 inches. A heat treat condition is not specified and the hardness range specification can be characteristic of both $^{1}/_{8}$ and ¼ hard conditions. Properties of all tubes tested were within specification.

Metallographic analysis could not conclusively determine a specified limit to number of bends allowable. A statistical analysis suggests a range of 5-7 bends with a 99.95% confidence limit. See the "Statistical Analysis" section of this report.

Background: The initial phase of this study involved two separate sets of test specimens. The first group was part of an investigation originating in the ESA-GTS [now Gas Transfer Systems (W-7) Group]. After the bend cycle test parameters were chosen (all three required bends subjected to the same amount of bend cycles) and the tubes bent, the investigation was transferred to Terri Abeln (Metallurgical Science and Engineering) for analysis. Subsequently, another limited quantity of tubes became available for testing and were cycled with the same bending fixture, but with different test parameters determined by T. Abeln.

Bending Procedures and Observations: The equipment used for both sets of tubes involved an aluminum mock with W76 bend tooling, provided and owned by BWXT/Pantex. The tube was attached to the mock by welding a threaded boss onto the tube that fit into a receiver in the mock. A bend cycle is defined as one bending operation followed by a straightening operation (each

requiring a different set of tooling). See Figure 1. The first set of tubes, 18 total, underwent all three bends.

The first set of tubes were also pressure tested after 15 bends to 10,000 psi and held for 5 minutes, except for tube #'s 18 and 19. All tubes were tested until failure, except for tubes #'s 11, 18, and 19, which were only subjected to 15 bends each. See Figure 2.

Tube failures were characterized as complete transverse separation or fracture through the tube wall thickness compromising functionality. It was noted in the first set that all the tube failures occurred at the third bend (180 degrees, 14.29 radius), in the inner radius area, during straightening. See Figure 3. Therefore, considering the limited amount of tubing available at the time, the second set of tubes, 21 total, were cut to 8 inch lengths and subjected to the third bend only. Fifteen tubes were subjected to 1 through 5 bends; three tubes per bend cycle. Five more tubes were given 6, 7, 8, 9, and 10 cycles. One tube was taken to failure and one non-cycled tube was used as a control specimen. See Figure 4. The second set of tubes was visually examined at 1X magnification for obvious fractures after every bend, as may be done during actual assembly and disassembly at Pantex. Fractures were not apparent before catastrophic overload.

Refer to Tables 1a and 1b for test parameters and results for both groups of specimens.

TABLE 1a

First Set (conducted by Al Bateman (retired) under the direction of Patti Buntain (W-1):

Tube #	# Bend Cycles*	Results
1	19	Single- wall fracture
2	26	Completely fractured
3	24	Completely fractured
4	27	Completely fractured
5	29	Single- wall fracture
6	25	Completely fractured
7	26	Completely fractured
8	23	Completely fractured
9	22	Completely fractured
10	19	Not submitted to T. Abeln
11	unknown	No obvious fracture (@1X)
12	22	Completely fractured
13	24	Completely fractured
14	26	Completely fractured
15	18	Completely fractured
16	25	Completely fractured

Tube #	# Bend Cycles*	Results
17	23	Single- wall fracture
18	15	No obvious fracture (@1X)
19	15	No obvious fracture (@1X)
No control sample submitted	---	---

** Cycle defined as one bending and straightening*

TABLE 1b

Second Set (conducted by Kathy Chilcoat (ret.) and Terri Abeln (under the direction of T. Abeln)

# of tubes bent to # of cycles*	Results
Three tubes bent to 1 cycle	No obvious fracture (1X)
Three tubes bent to 2 cycle	No obvious fracture (1X)
Three tubes bent to 3 cycle	No obvious fracture (1X)
Three tubes bent to 4 cycle	No obvious fracture (1X)
Three tubes bent to 5 cycle	No obvious fracture (1X)
One tube bent to 6 cycles	No obvious fracture (1X)
One tube bent to 7 cycles	No obvious fracture (1X)
One tube bent to 8 cycles	No obvious fracture (1X)
One tube bent to 9 cycles	No obvious fracture (1X)
One tube bent to 10 cycles	No obvious fracture (1X)
One tube bent to complete fracture: 28 cycles (F28)	---
One tube used as Control Specimen	---

** Cycle defined as one bending and straightening*

Fractography and Scanning Electron Microscopy (SEM) Analysis: Fractography, using SEM and light microscopy, revealed a fracture mode characteristic of multiple initiation, low cycle fatigue (LCF). There are three stages of fatigue: initiation, propagation, and overload. See Figure 5. All fracture surfaces exhibited an initiation site associated with the exterior surface of the tube, at the inner bend radius area of the third bend location. See Figure 6. Ratchet marks were evident at low magnification (Figure 6) and characteristic of multiple crack initiation and propagation. Cyclic arrest marks (also called clamshell or beach markings), characteristic of fatigue, were evident and indicative of crack propagation primarily in planes normal to the bending load. See Figure 7. The determinable number of markings was closely associated with the number of bend cycles. Both macro features (ratchet and cyclic arrest marks) pointed to a common initiation site on the fracture surface. The overload region exhibited both tensile and shear ductile dimples. See Figure 8. Features in the sidewall region indicated some torsional loads also. Macrofractography suggests that catastrophic failure occurs when ½ to ¾ of the tube wall is compromised via crack propagation and wall thinning resultant of plastic deformation (necking). See Figure 9. SEM surface and cross-sectional analysis revealed that cracks initiated

during the first bend cycle. Figures 10 and 11 illustrate surface initiated cracks in tubes subjected to differing numbers of bend cycles. Figure 12 shows apparent differences in the pre-test surface condition of all submitted tubes. Some circumferential, oval distortion was noted with a nominal aspect ratio (side diameter to bend radii diameter) of ~1.25.

Material Characterization and Analysis: According to reported Rocky Flats specification P14548, seamless tubes were fabricated out of type 304 VIM-VAR stainless steel bar (Rocky Flats specification P14510) and measured 0.125 (+0.003) inches in diameter with a wall thickness of 0.028 ($\pm$0.0015) inches. Specimens from each tube were metallographically prepared to reveal transverse and longitudinal cross-sections in polished and electrolytically etched conditions. Transverse cross-sections in non-deformed regions revealed tube diameters and wall thicknesses to be within specification. Depth of cracks and inclusions were analyzed in the polished condition, while other microstructural information (grain boundaries, twinning, alloy phases, etc.) was revealed after etching. Light microscopy revealed an etched microstructure consisting primarily of the austenite phase with little to no ferrite phase present. Twinning, due to heat treatment and deformation, was observed in all tubes including the control sample. See Figure 13. Microstructural characteristics indicating deformation were observed in larger degrees with increasing bend cycles. The inner radius wall exhibited more deformation than the outer radius wall. All cracks were transgranular in nature, another characteristic of LCF. See Figures 14 and 15. Microstructural ferromagnetic character, which can be indicative of deformation martensite (α') formation (from the austenite phase; $\gamma \rightarrow \alpha$'), was measured using a commercially available Ferritescope equipped with a two-point probe. Larger quantities were measured in the bend areas as compared to undeformed areas of the tube, but comparison of measurements in tube areas subjected to differing numbers of bends was inconclusive. Deformation martensite was not visually discernible in the tube microstructures using available metallography laboratory light microscopy and SEM instruments.

A specific heat treat condition was not included in the tubing specification. The applicable bar stock specification dictates the material to be treated to an annealed condition. The hardness range required by the tubing specification is 200 – 300 KHN which translates to ~HRB89 –

HRC29. This hardness range is indicative of both 1/8 hard and ¼ hard heat treat conditions. Hardness measurements on the control sample tube (that was not subjected to bending) averaged HRC 22. Measurements on several tubes in the third bend location were as high as HRC 40. Grain size was also not specified in the tubing specification, but required to be ASTM 5 or finer in the bar stock specification. Grain sizes were measured to be in the range of ASTM 4.5 to 5.5.

Allowable tube defects in both the outside surface and tube wall (ultrasonic inspection) were specified to be less than 0.002 inches in depth by 0.030 inches in length. Metallographic cross-sectional depth measurements of defects or cracks nearing the dimensions allowed by specification were not observed until the 15th bend cycle (maximum measurement was ~0.002 inches in depth). Cracks at 5 and 10 bend cycles measured to be as much as ~0.0003 inches and 0.001 inches in depth, respectively. See Figures 16 and 17. The deepest cracks were always observed propagating from the tube exterior surface associated with the inner bend radius, with more shallow cracks in the outer bend radius. No cracks were observed on the interior surfaces of the tubes when examined up to a maximum magnification of 1000X. Chemical composition limits were found in two specifications cited in RF tube specification P14548, RF bar stock specification P14510 and AMS 5560. Samples of two tubes from Set 1 and the one failed tube from Set 2 are compared with the specification limits in the following Table 2:

TABLE 2

Element (Wt %)	Tube Set 1 - #5	Tube Set 1-#15	Tube Set 2-#F28	P14510	AMS5560
C	0.064	0.066	0.062	0.05-0.07	0.08 max
Mn	1.550	1.550	1.530	1.5-2.0	2.0 max
P	0.012	0.013	0.011	0.02 max	0.04 max
S	0.002	0.003	0.003	0.01 max	0.03 max
Mo	0.016	0.016	0.015	0.2 max	0.75 max
Si	0.520	0.510	0.500	0.3-0.6	1.0 max
Al	0.002	0.002	0.003	0.03 max	---
Co	0.031	0.032	0.030	0.20 max	---
Cu	0.034	0.032	0.030	0.30 max	0.75 max
N	0.015	0.016	0.015	0.01 max	---
O	0.0057	0.0046	0.0057	---	---
H	0.0007	0.0010	0.0008	---	---

Methods: Oxygen, Nitrogen, and Hydrogen – Inert gas fusion
Carbon and Sulfur – Combustion infrared detection
All others – Direct current plasma emission spectroscopy

One inclusion, of considerable size, was revealed in metallographic longitudinal cross-section in Set 1 – Tube #11. The inclusion measured a little over 0.002 inches long by 0.0002 inches in width, with its length in parallel to crack propagation. The location of the inclusion was in the larger bend radius wall, not the smaller bend radius where cracks initiate. Chemical analysis of the inclusion, using Energy Dispersive Spectroscopy (EDS), revealed a predominate peak signal characteristic of silicon. Because the inclusion did not lie in the direction of tube working, i.e., drawing, it was suspected to be brittle in nature. See Figure 18.

Terri Abeln performed all metallographic characterization.

Observations and Conclusions:

In all cases, the mode of failure was multiple initiation, very low cycle fatigue. Every failure was located in the 3rd bend area of the tube (reportedly 180 degree bend angle and 14.29 bend radius), with initiation on the exterior surface of the bend inner radius. According to the science of fracture mechanics, this type of bending mode detects crack initiation on exterior surfaces. The combination of bend angle and bend radius at the 3rd bend location promotes the most severe stress state and justifies first failure in this area. In other words, concentration of stress is increased with increasing bend angle and decreasing bend radius. The number of bend cycles to failure ranged from a minimum of 18 to a maximum of 29. The maximum allowable flaw size occurs after the 15th bend cycle. Out of 39 tubes examined, an inclusion was found with its ~0.002 inch length oriented parallel to planes of fracture. If fatigue propagation had encountered this inclusion, the actual number of bends to failure may have been affected significantly (0.002 inch cracks were observed after the 15th cycle). In low cycle fatigue, at these high stress levels, the second stage of fatigue, *propagation*, dominates the tube lifetime, not the first stage, *initiation*. Mechanical properties and microstructural characteristics dictate lifetime more than surface characteristics. The important thing to note is the depth of penetration into the wall when catastrophic failure occurs. Unfortunately, crack propagation depth was observed to be anywhere from ½ to $^{3}/_{4}$ of the wall thickness, taking into account appreciable necking. While the bending operation is somewhat controlled, the straightening operation is far from controlled. Many variables exist in the bending cycle. Material “springback”, operator “tweaking” and ambiguous procedures are some of the causes. During the straightening operation, the load is distributed, but not uniformly, and distributed differently from bend cycle to bend cycle. This load variability,

along with possible material variability, results in the observed large variation in number of cycles to failure and crack propagation depths to catastrophic overload. Pressure testing of the tubes produced negligible effects on bending dynamics.

Comparisons and Comments with Previous Tube Bending Reports:

Mechanical Properties and Surveillance of the W-- Pit Tube in Stockpile, P.E. Terrill Lawrence Livermore National Laboratory (LLNL)

- May 26, 1999.
- Tested with 90 degree bend for third bend (not the required W76 third bend)
- No tooling radius was reported
- Reportedly used tubing ordered via the same RF specification as this present LANL study
- 14 tubes taken to failure
- Minimum of 13 bend cycles, maximum of 17 bend cycles
- No micro-cracks in 0-3 bends, .001 in (6 bends) .006 in (7 bends)
- "...95% sure that ultimate failure will not occur prior to the 6^{th} bend (less than 0.001% chance of failure) ...surface micro-cracks were initiating on 6^{th} straightening cycle."

Comments: Terrill's study reports third bend testing with a less severe angled bend than in this present LANL study, but important information in bend tooling radius and load distribution dictated by the straightening operation used in Terrill's study was not reported, therefore inhibiting stress state comparisons. In contrast to Terrill's study, this present LANL study revealed exterior surface cracks after 1 bending operation

Characterization of Stainless Steel 304 Tubing, A.J. Sunwoo, M.A. Brooks, J.E. Kervin (LLNL)

- October 16, 1995
- Reportedly used tubing ordered via the same RF specification as this present LANL study
- Used tooling with a 90 degree bend for third bend (not the required W76 third bend)
- No tooling radius was reported
- Reported that a statistical study produced a 95% confidence level at 5 bends (additional to present state of tubes)
- For a 99.99% confidence level, would expect failures to occur between 19 and 31 cycles and then using a safety factor of 2, resulting in 9 cycles
- "lifetime dominated by crack initiation and following initiation, the tubes proceed quickly to failure"*
- 6 inch specimens
- 4 tubes taken to failure

- Minimum of 13 bend cycles, maximum of 16 bend cycles
- Appeared to be no micro-cracks after 5 bends
- "Following the initiation of cracks with lengths of about 10 – 20 microns, propagation failure occurs quickly in just a handful of bends."**

Comments: As in Terrill's, Sunwoo's study reports third bend testing with a less severe angled bend than in this present LANL study, but important information in bend tooling radius and load distribution dictated by the straightening operation used in Sunwoo's study was not reported, therefore inhibiting stress state comparisons. More test tubes may have been needed for a better statistical study.
** This statement is incorrect in a low cycle, (high stress) fatigue mode of failure... lifetime is dominated by the propagation stage.*
*** This statement is also incorrect for the same reason and non-definitive as to the relation to the bending lifetime.*

LLNL Pit Tube Bending Limits, H.L. Flaugh, J.J. Petranto (LANL)

- January 28th, 1991
- Purpose was to investigate bending limits for LANL/LLNL annealed tubing
- Used ¼ hard LLNL tubing for test
- Bent up to 11 cycles with completely reversed bending
- Same tube dimensions as in this present LANL study
- 90 degree bend, around a 1.0 in OD rod (not the required W76 third bend)
- Used tube bender in test
- Conclusion: "no practical limit and without degradation"

Comments: Flaugh's study used quarter–hard condition tubing for an annealed condition study. He also completely reversed the bending operation instead of just straightening the tube. Flaugh reportedly used a tube bender, which uniformly distributes the load, thus lowering the concentration of stress and increasing bending lifetime. Both the bending angle and bending radius in Flaugh's study were less severe as in this present LANL study.

Statistical Analysis: The following is a statistical analysis graph and table provided by David Jarboe of Honeywell / KCP.

Graph 1

Graphical representation of failure prediction based on Weibull distribution. The middle line is the regression fit to the actual data points (triangles).

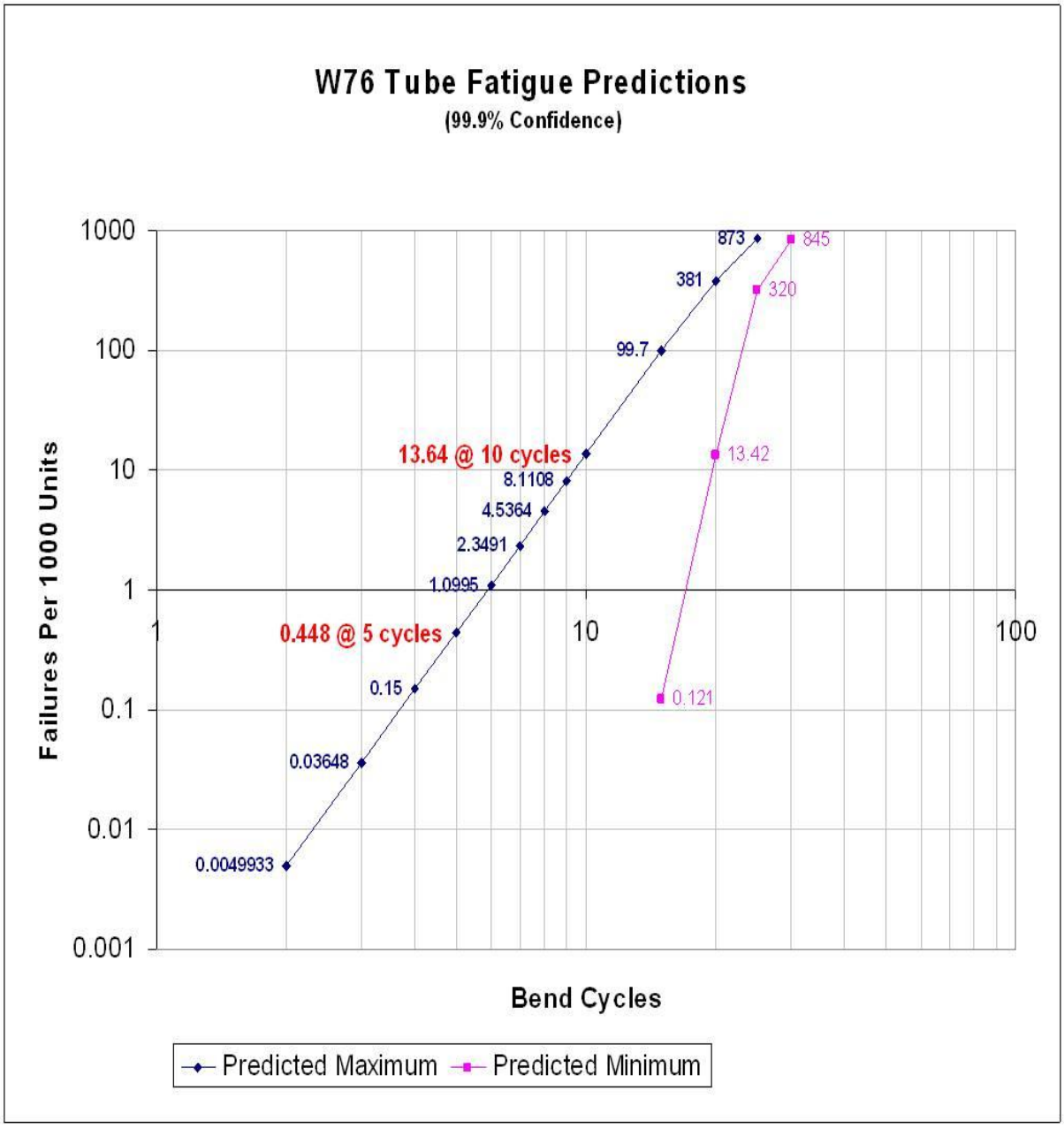

Table 3
Calculated data from WinSMITH™ Software

Occurrence (Parts per 1000)	99.5% Lower Limit (Cycles)	Regression Fit to Data (Cycles)	99.5% Upper Limit (Cycles)
0.1	4.624	8.442	15.41
0.2	5.249	9.176	16.04
0.3	5.653	9.634	16.42
0.4	5.958	9.973	16.69
0.5	6.206	10.240	16.91
1.0	7.044	11.130	17.60
1.5	7.585	11.690	18.02
2.0	7.994	12.100	18.32
2.5	8.325	12.430	18.56
3.0	8.607	12.710	18.76

***Author Recommendations*:** Due to the inherent, uncontrolled nature of the straightening operation, a metallurgical analysis is inconclusive when predicting an accurate tube-bending lifetime. Another study or "second phase" of this study is required to not only establish a "worst case" baseline for lifetime analysis, but as a reference in the study of possible predisposed defects during tube lifetime.

A "Second Phase" study should:

- Incorporate modeling for future studies
- Induce known defects
- Incorporate surface effects
- Correlate mechanical properties and microstructure
- Understand and employ control samples
- Go from distributive load to point load for worst case scenario.

Assessing the condition of the tube and remediation:

- Eddy current / UT testing for critical crack length
- Recovery of the tube microstructure via localized induction heating.

Acknowledgements:

- Patti Buntain: W-1/LANL
- Al Bateman: Retired/LANL
- Kathy Chilcoat: Retired/LANL
- Dave Jarboe: Honeywell/KCP
- Stephen P. Abeln: AET-5/LANL
- Geoff Brown: MST-8/LANL
- Pat Dickerson: MST-6/LANL
- Pallas Papin: MST-6/LANL

References

1. *Effects of Strain State and Strain Rate on Deformation-Induced Transformation in 304 Stainless Steel: Part 1. Magnetic Measurements and Mechanical Behavior*, S.S. Hecker, M.G. Stout, K.P. Staudhammer, and J.L. Smith. (1995).
2. G. F. Vandervoort, *Metallography- Principles and Practice* (1984).
3. ASM Handbook, Volumes 11 and 19, Tenth Edition (1992).
4. ASM Specialty handbook, *Stainless Steels*, (1994).
5. D. Hull, *Fractography,* (1999).
6. *W76 Pit Tube Fatigue Life: Statistically Based Bend limit Recommendation*, D. M. Jarboe (2003).

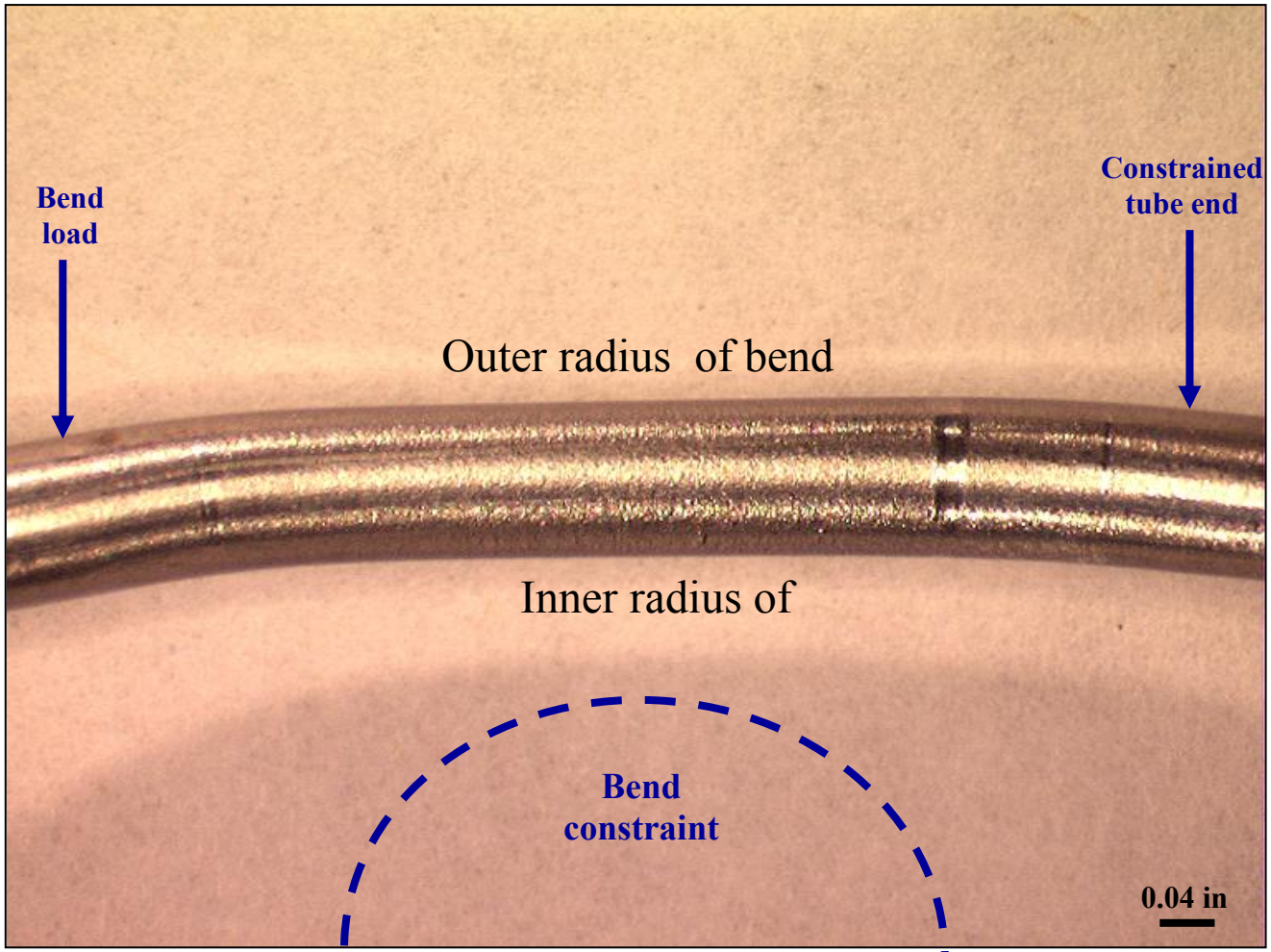

Figure 1 – Photo illustrating bend load and constraints using tube #18 (1st group / 15 bend cycles).

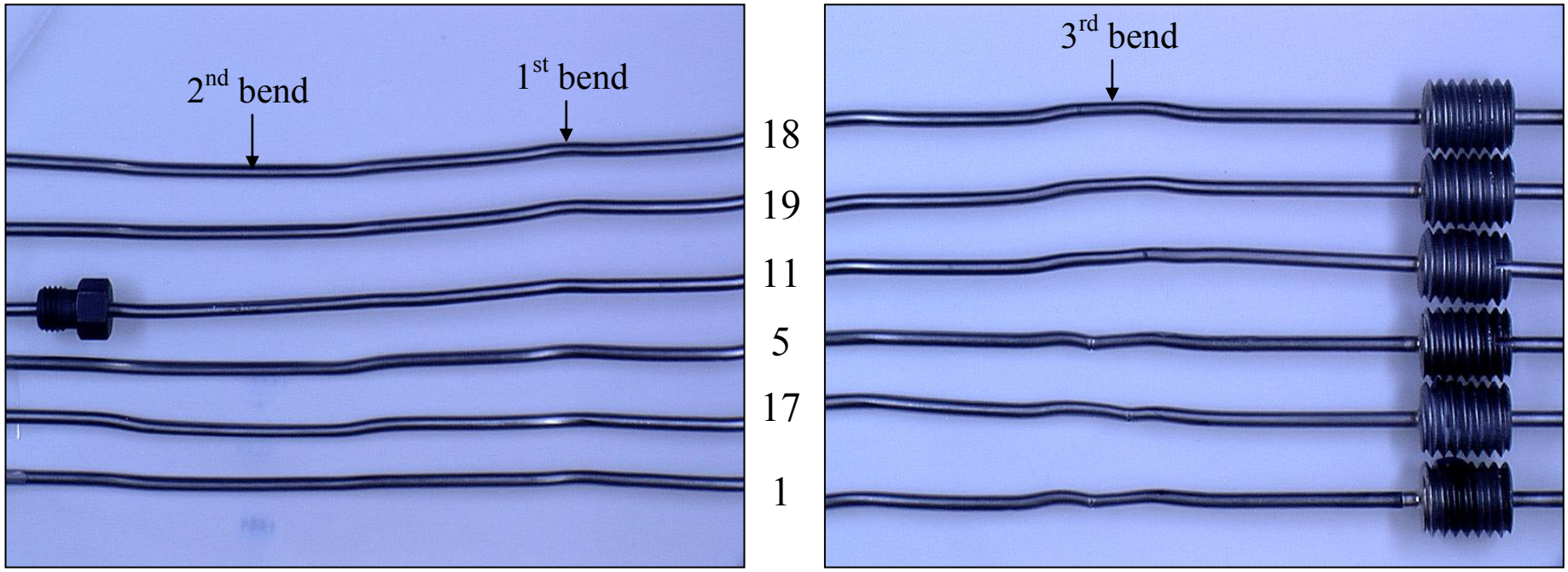

Figure 2 – Overall photos of 6 submitted tubes from 1st set (#'s 5, 17, 1 with through wall fractures).*

Tube # 18 – bent and unbent 15 times (Not Pressure Tested)
Tube # 19 – bent and unbent 15 times (NPT)
Tube # 11 – bent and unbent 15 times (Pressure Tested**)
Tube # 5 - bent and unbent 29 times (PT)
Tube # 17 - bent and unbent 23 times (PT)
Tube # 1 - bent and unbent 19 times (PT)

Also submitted: 12 completely fractured tubes ranging 18 to 27 bends
****** Pressure tested to 10,000 psi and held for 5 minutes***

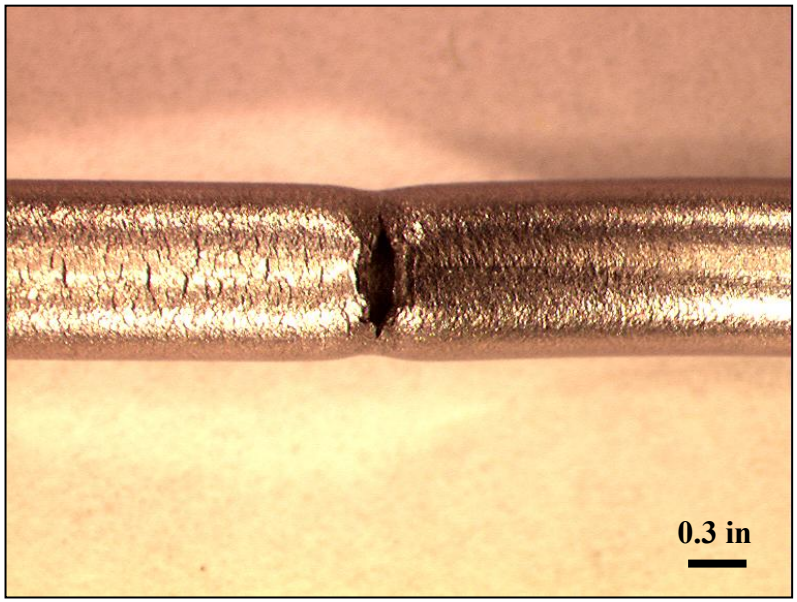

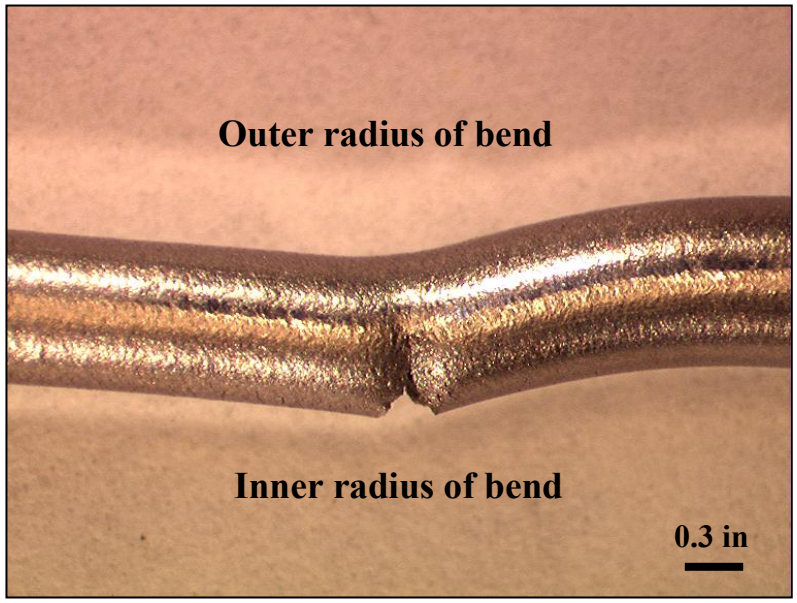

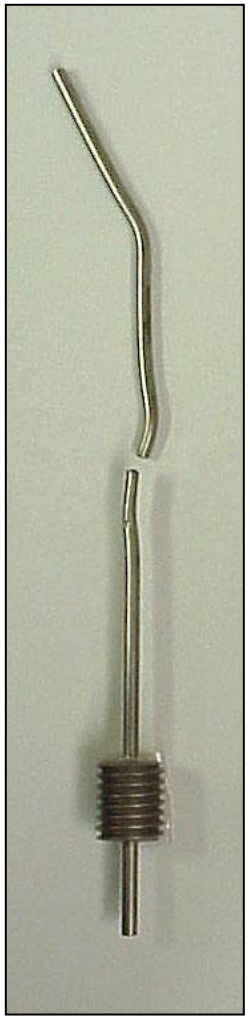

Figure 3 – Example photos of failures with complete fractures and single-wall fractures at third bend location.

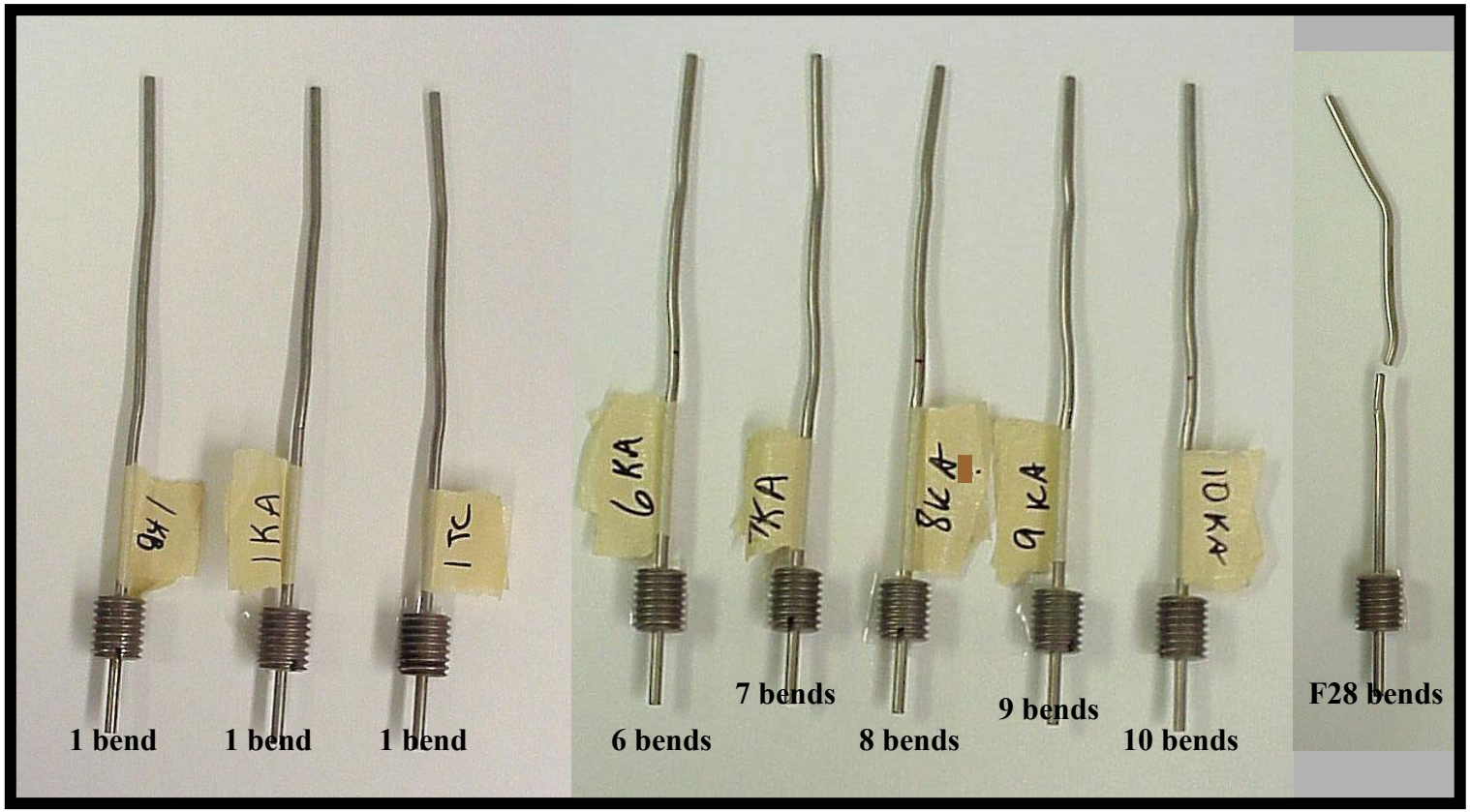

Figure 4 – Overall photo of some of the bent and straightened tubes from the second specimen group. The 3rd bend (see Figure 2) was the only one performed on this second group of tubes as it was determined to be the most critical bend.

Three Stages:
-Initiation
-Propagation
-Overload

Initiation: possible rubbing, possible ratchet marks
Propagation: cyclic arrest lines created if loading is interrupted or if stress amplitude changes

Overload: may contain shear lips depending on degree of constraint and inherent toughness
Size of fatigue and overload regions depend on nominal and local stress – high stress gives large overload region

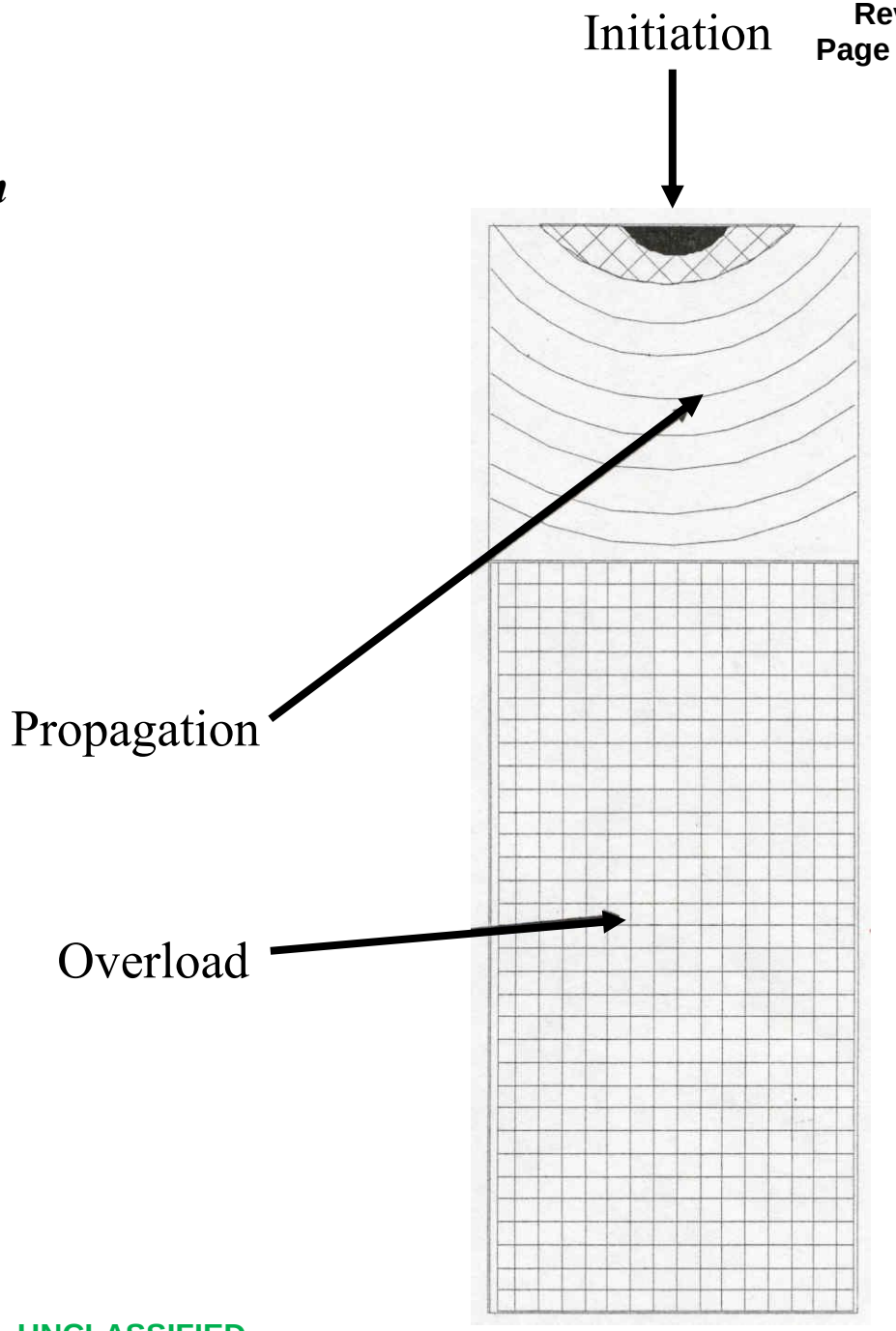

Figure 5 – Macro Fatigue

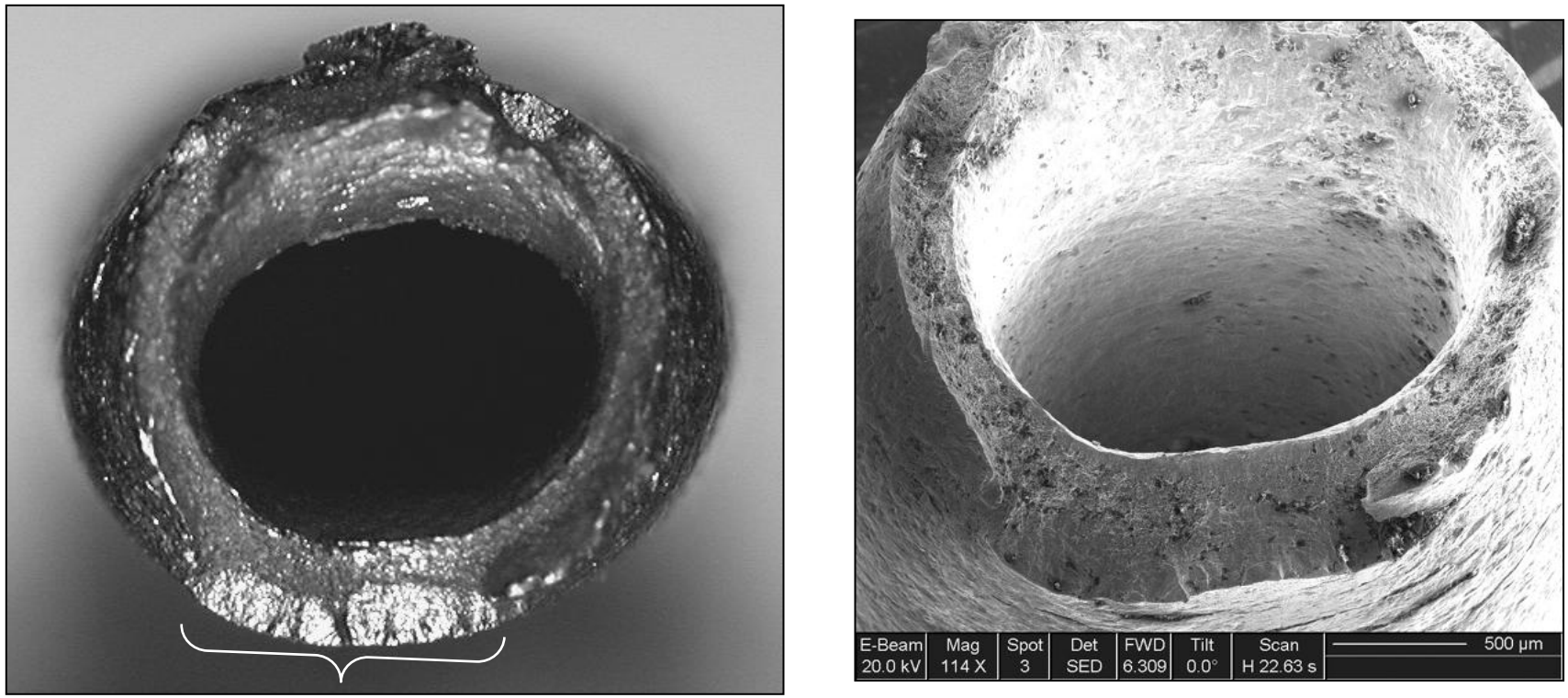

Figure 6 – Macro (left photo) and SEM fracture face photos of the failed tube from the second group of specimens (28 bend cycles). Fracture initiation sites illustrated with bracket.

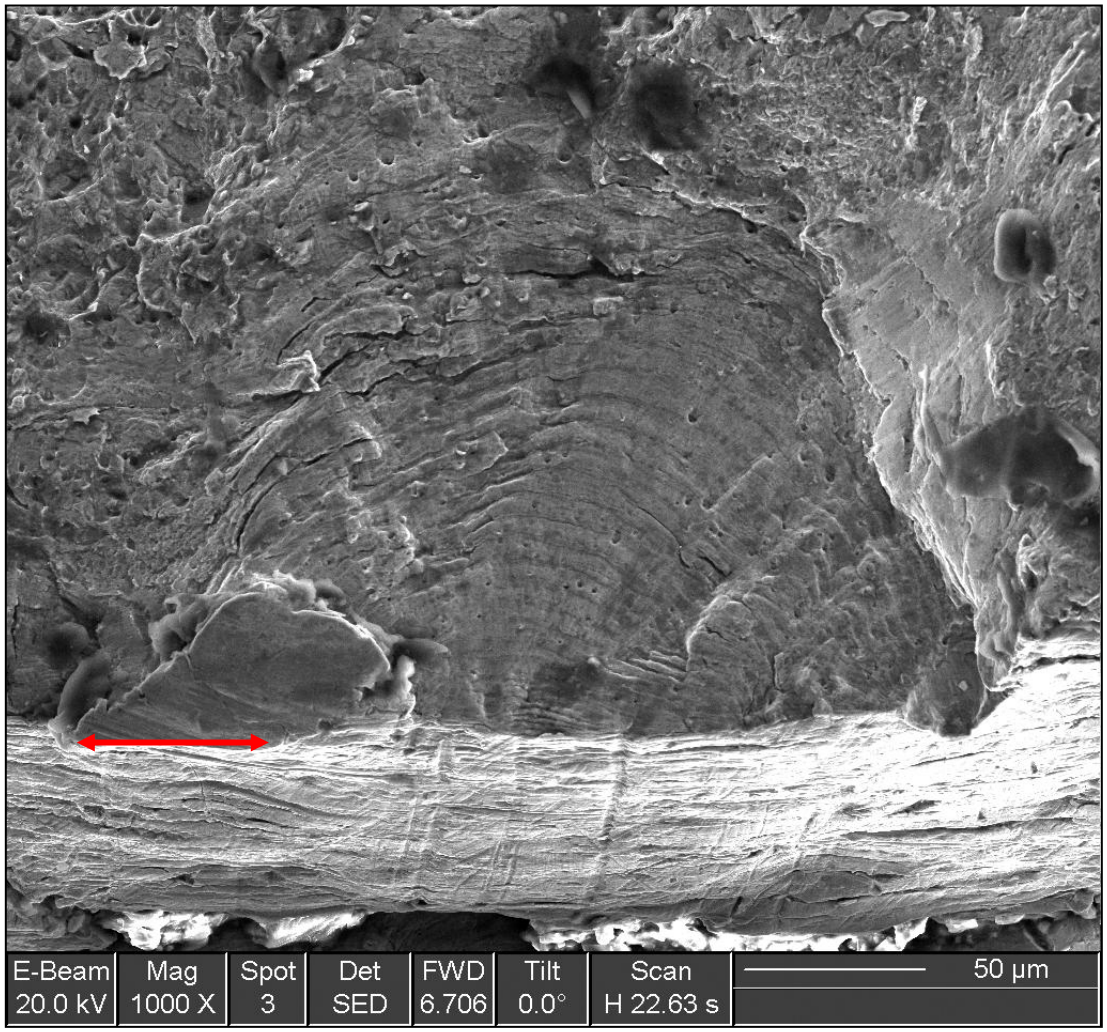

Figure 7 – SEM image of one initiation site on fracture surface of tube depicted in Figure 6. Note bend-induced cyclic arrest marks (clamshell pattern). Red arrows depict intersection of fracture surface and tube exterior surface.

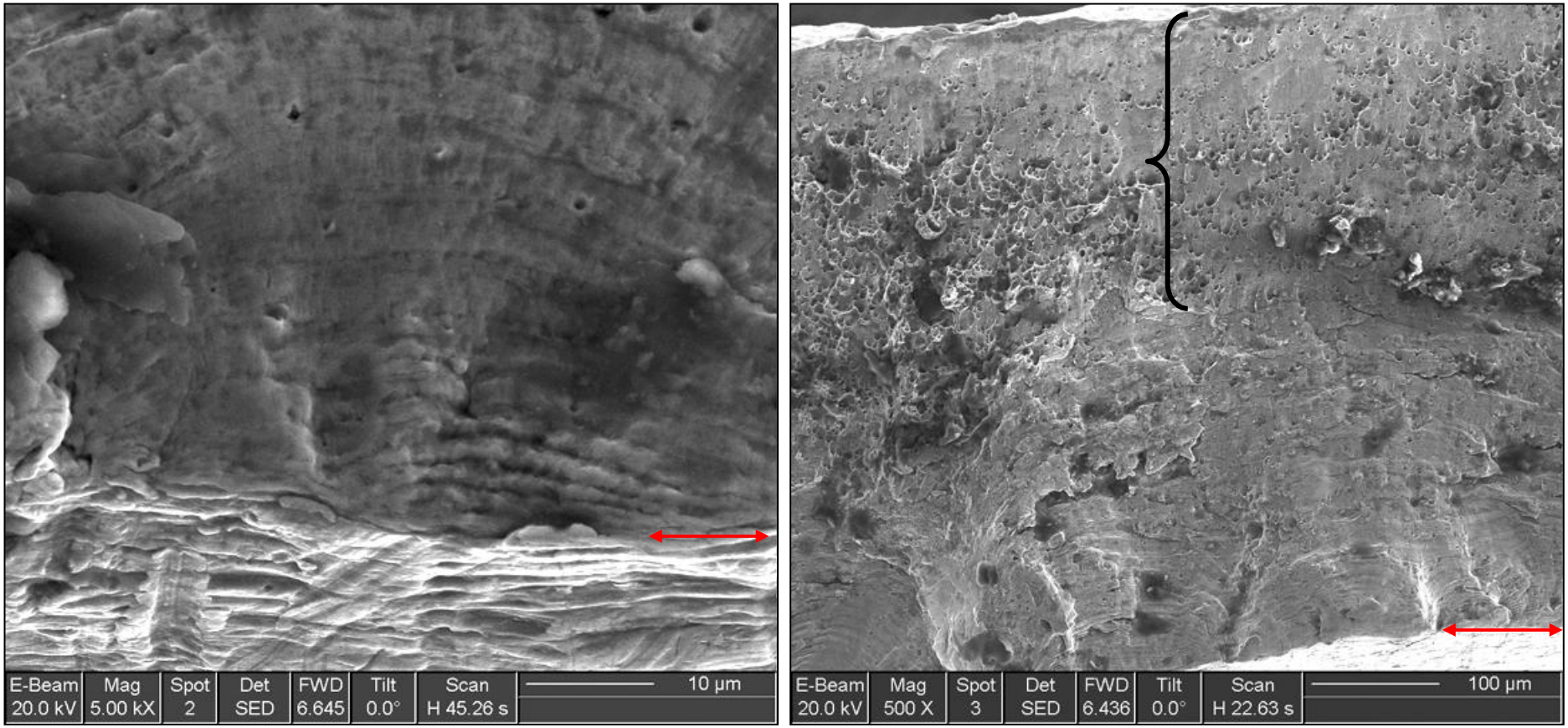

Figure 8 – Left image represents a higher magnification of the initiation site depicted in Figure 7 and right image is at lower magnification illustrating shear regions (bracket). Red arrows denote intersection of fracture surface and tube exterior surface.

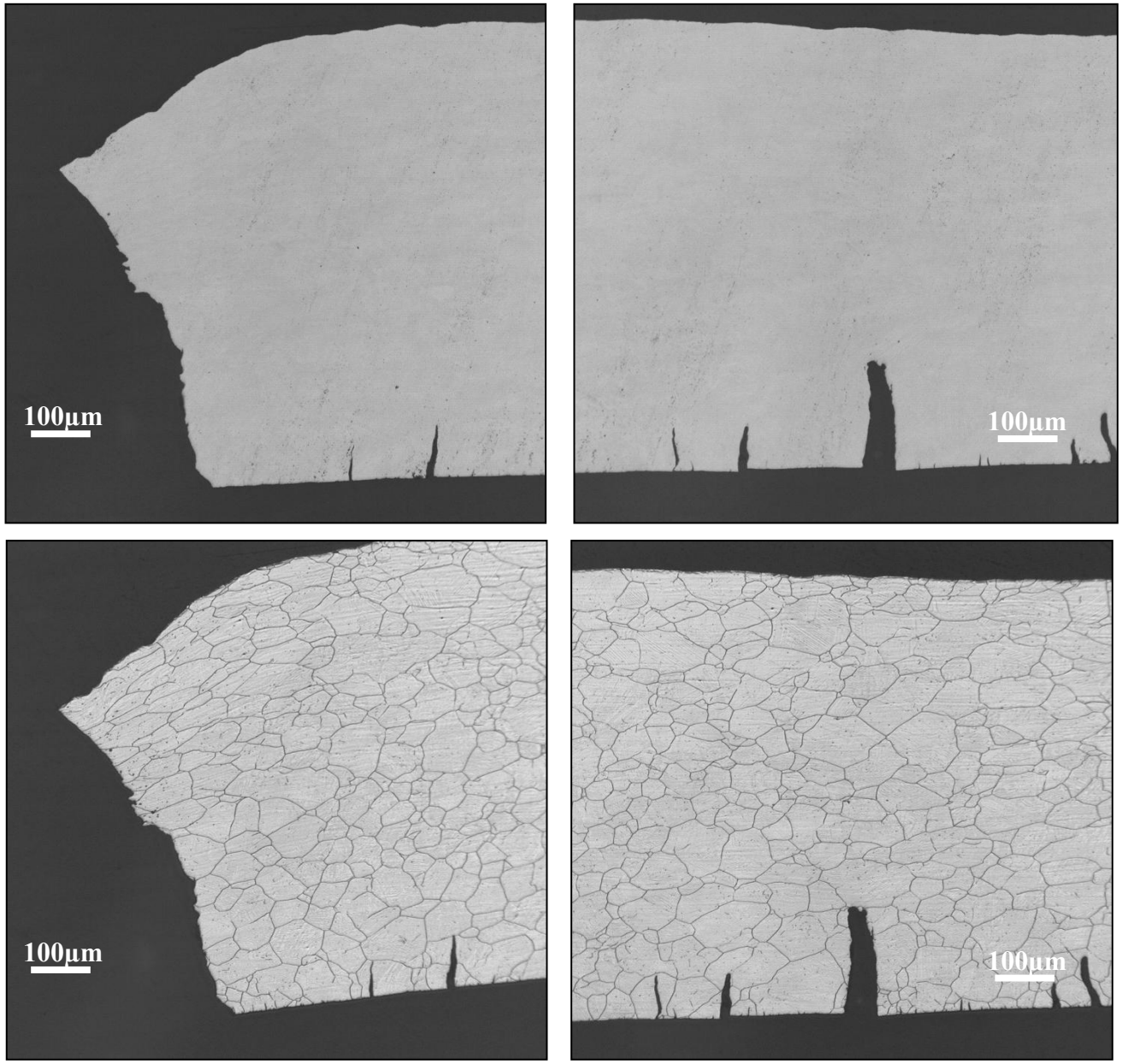

Figure 9 –
Photomicrographs of the polished and etched cross-sectional fracture area of the failed tube from group 2, 28 bend cycles. Etchant used was electrolytic nitric acid.

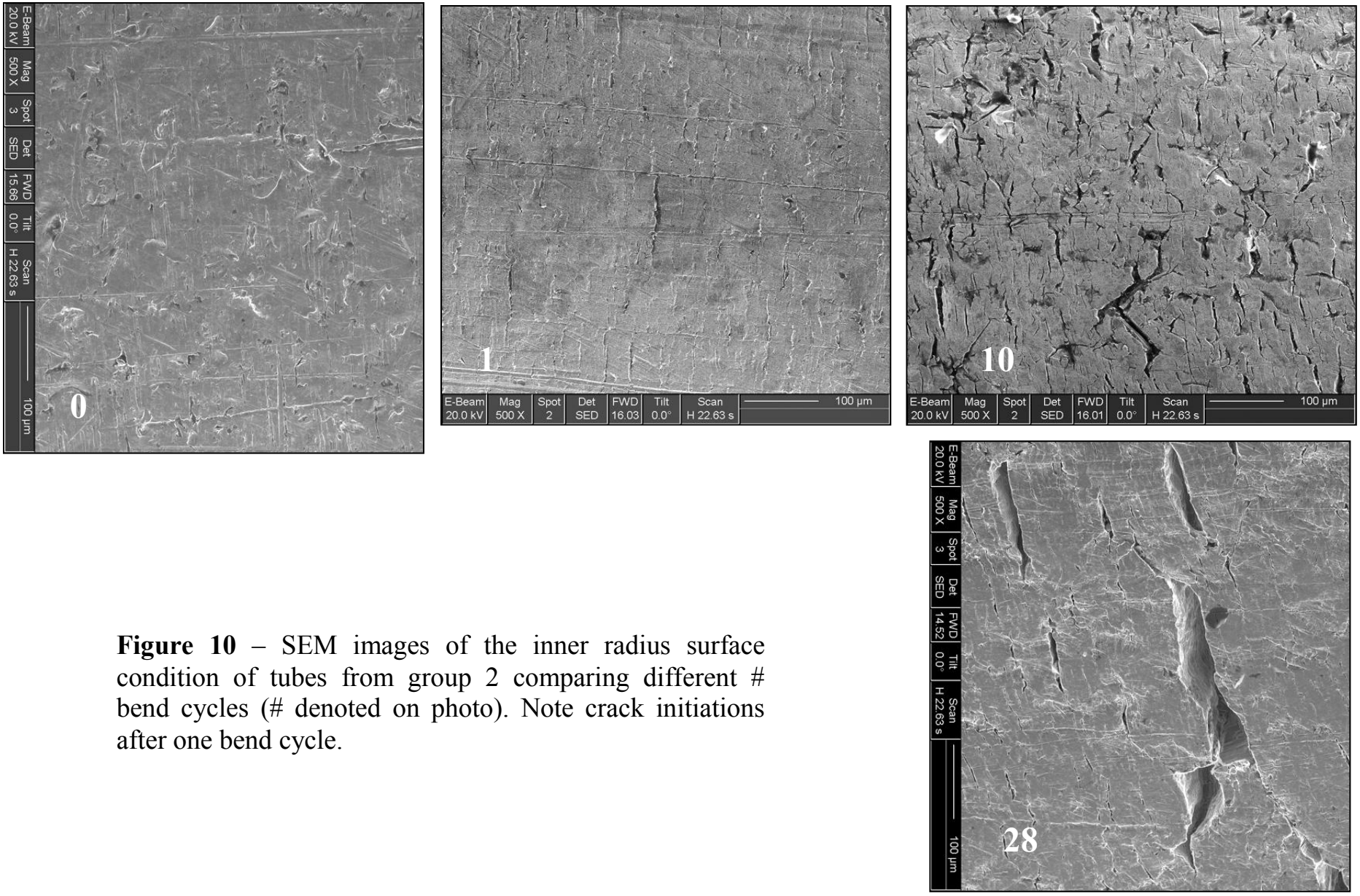

Figure 10 – SEM images of the inner radius surface condition of tubes from group 2 comparing different # bend cycles (# denoted on photo). Note crack initiations after one bend cycle.

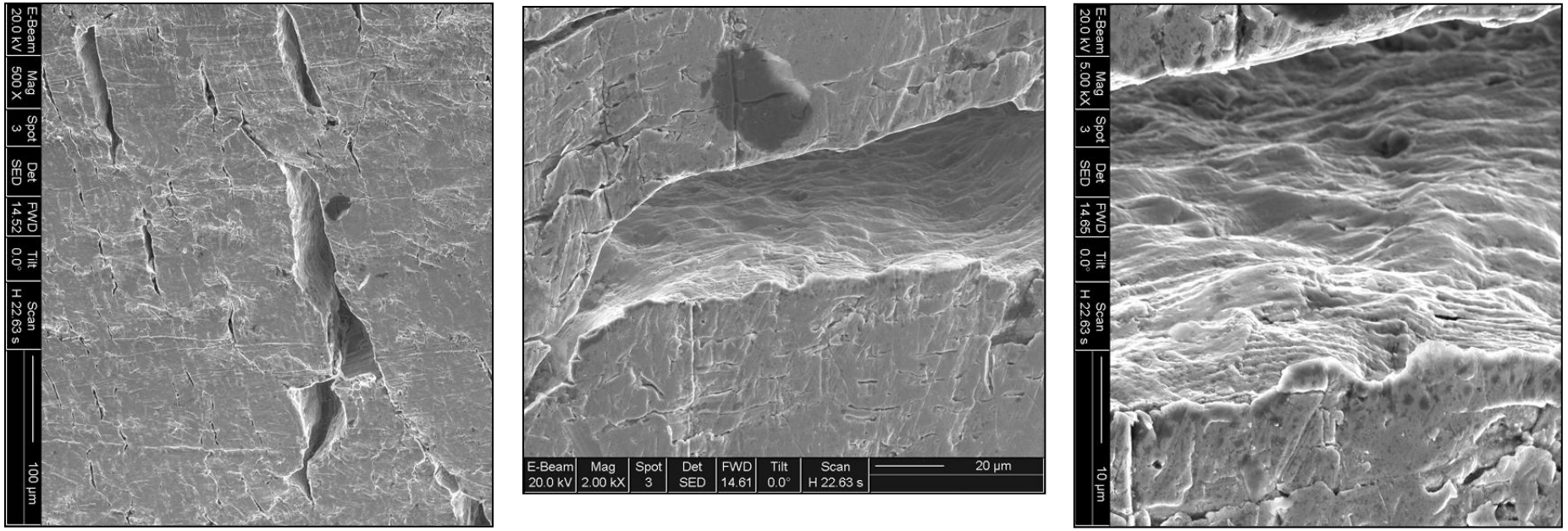

Figure 11 – Higher magnification SEM images of the surface condition of the 28 bend cycle tube surface depicted in Figure 10. Note cyclic arrest marks in right photo.

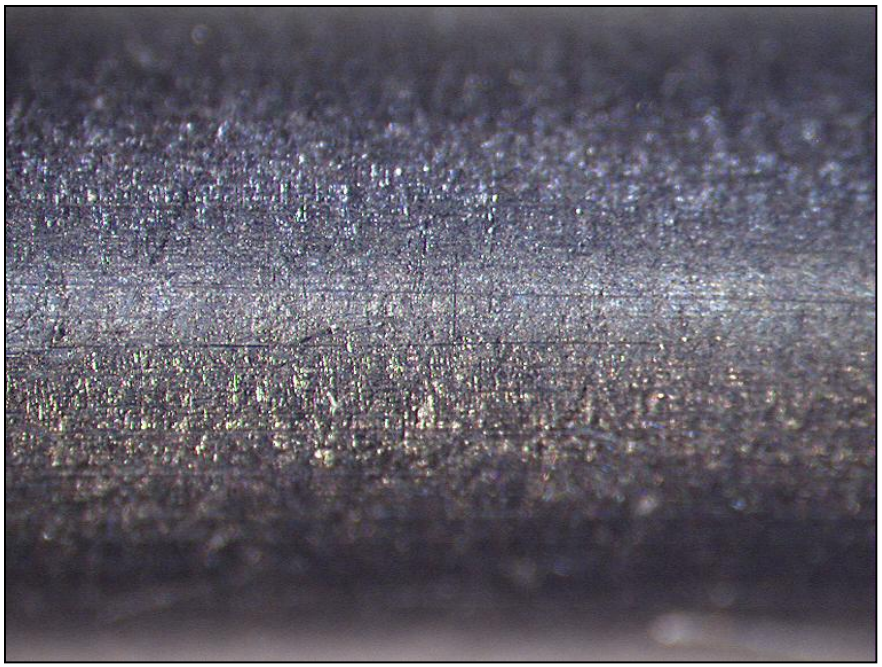

Tube 15 from group 1 (18 bend cycles)

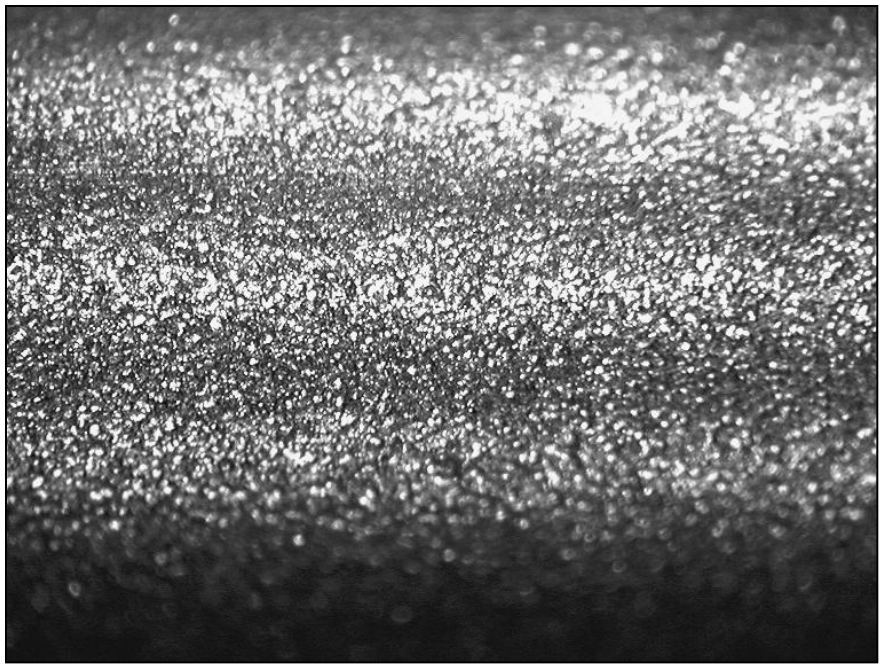

Fractured tube from group 2 (28 bend cycles)

Figure 12 - As-received tube surface conditions of two completely fractured tubes from both groups of specimens (originally photographed at 35X).

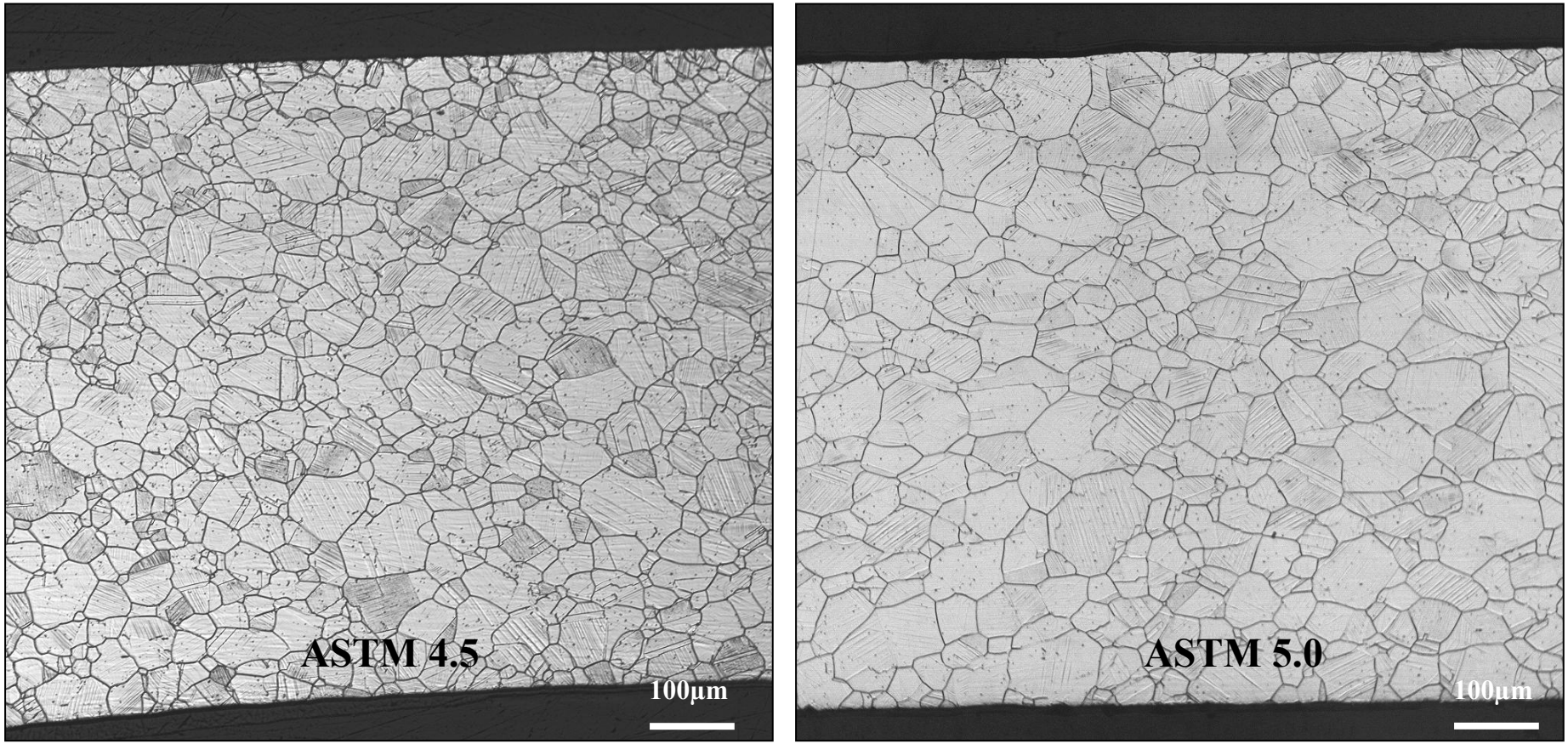

Figure 13 – Photomicrographs showing etched (electrolytic nitric acid) microstructural comparison between as-received (unbent) samples from the two groups of submitted tubes. Although no control tube was submitted in the 1st group, a section was examined that was adequately far away from the bend area and represented in the left photo. The right photo depicts the submitted control tube from the second group of tubes. There appears to be a similar amount of retained deformation but a difference in grain size (denoted on photo).

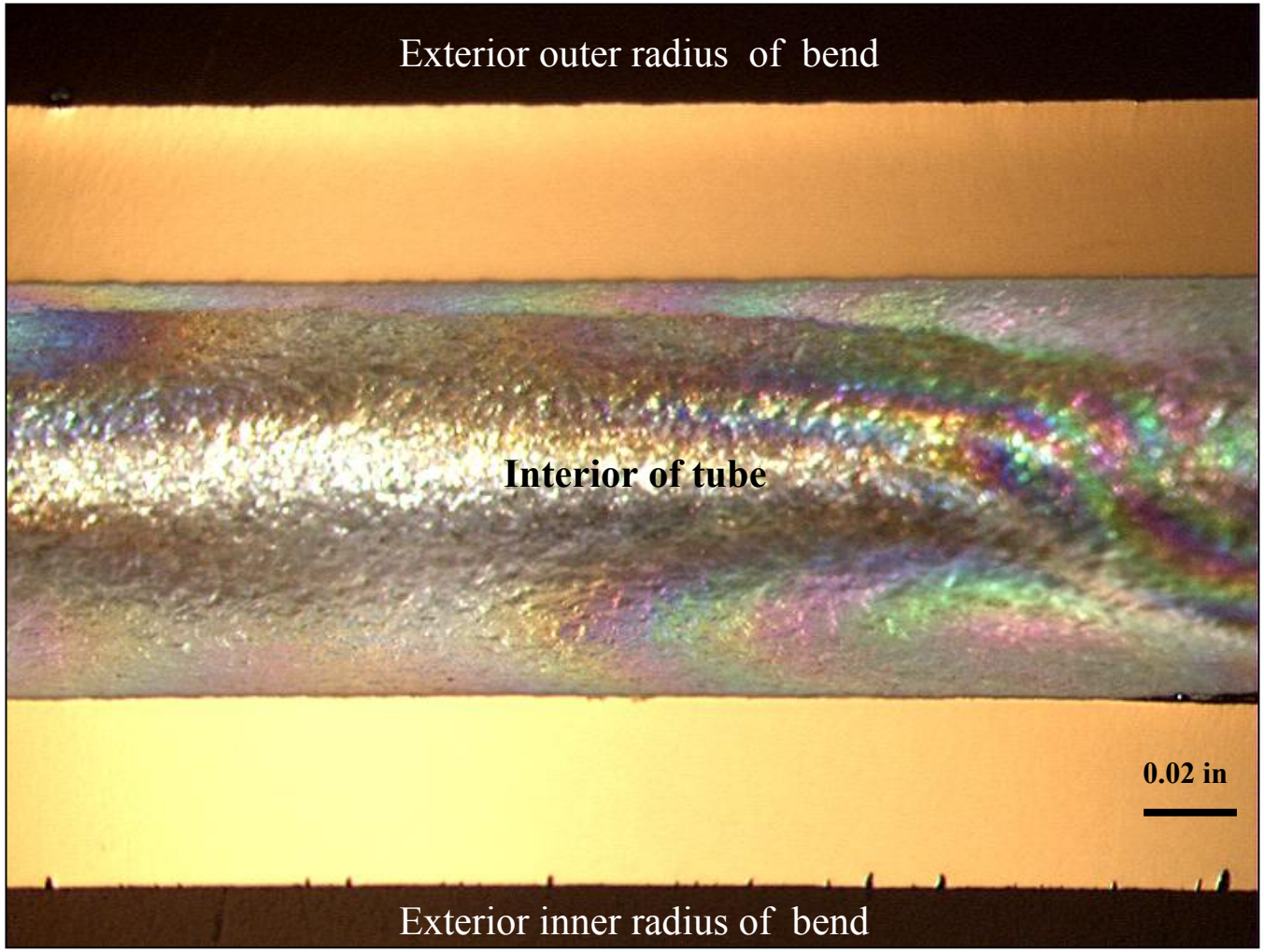

Figure 14 – Longitudinal cross-sectional view of tube #18 (group 1 / 15 bend cycles)

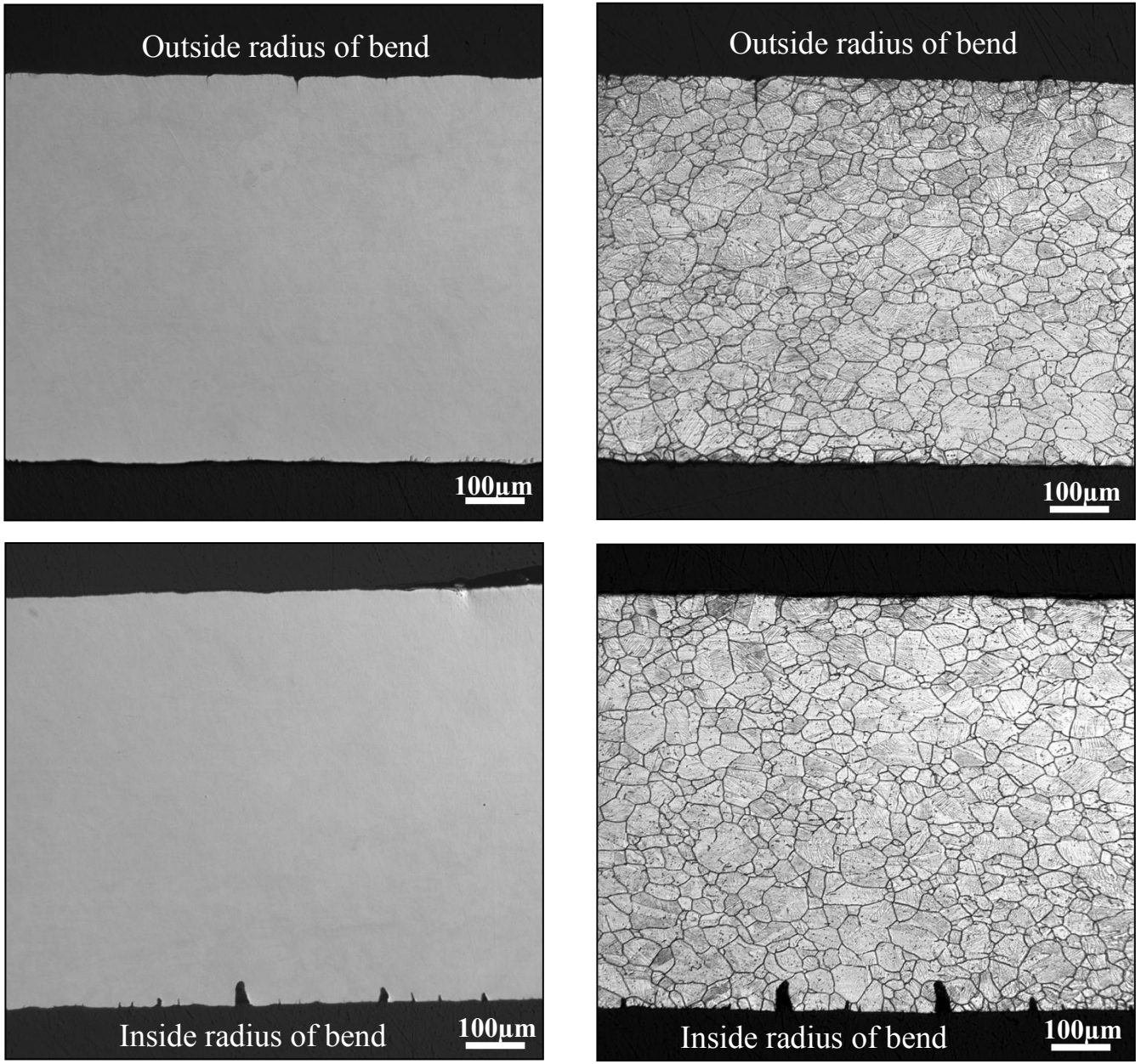

Figure 15 – As-polished and etched cross-sections of tube walls in tube #18 (group 1 / 15 bends). *Note that the two conditions were not photographed in the exact same areas.*

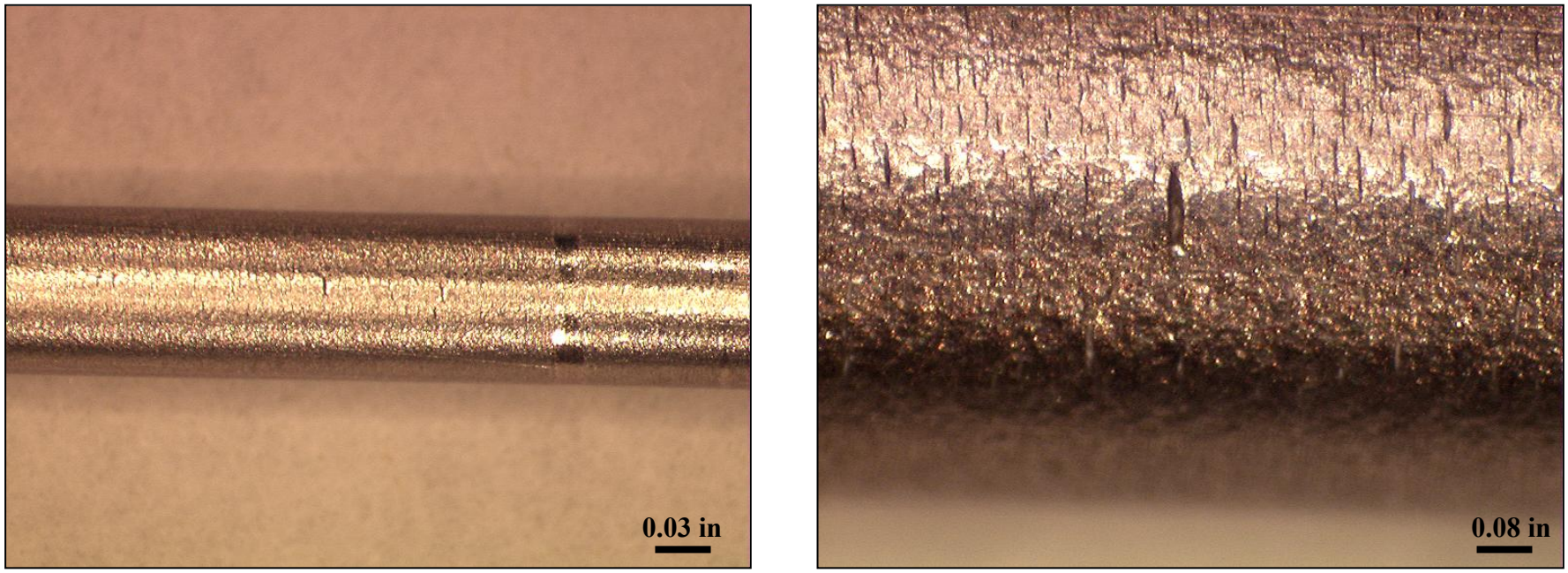

Figure 16 – Surface condition photos of tube #18 (group 1 / 15 bend cycles) inside radius of bend.

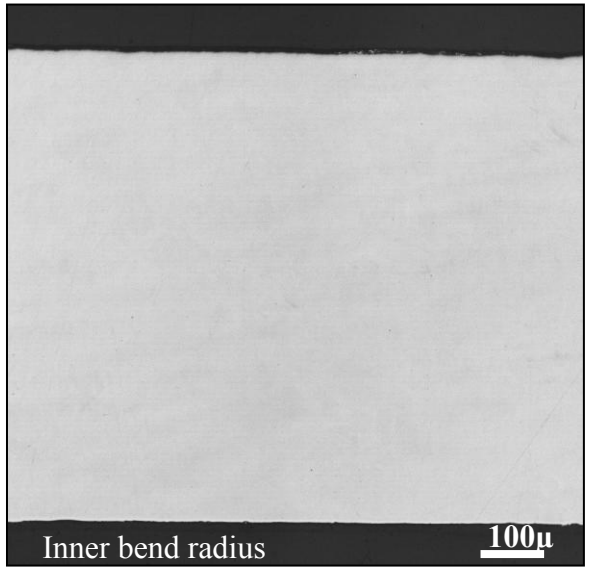

0 bend cycles

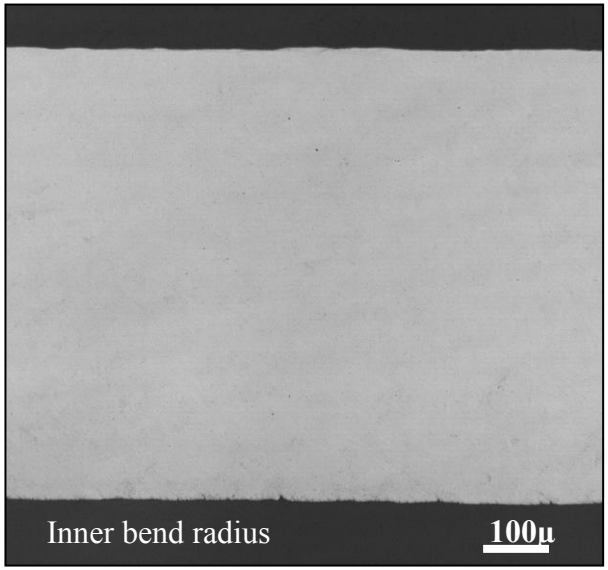

5 bend cycles

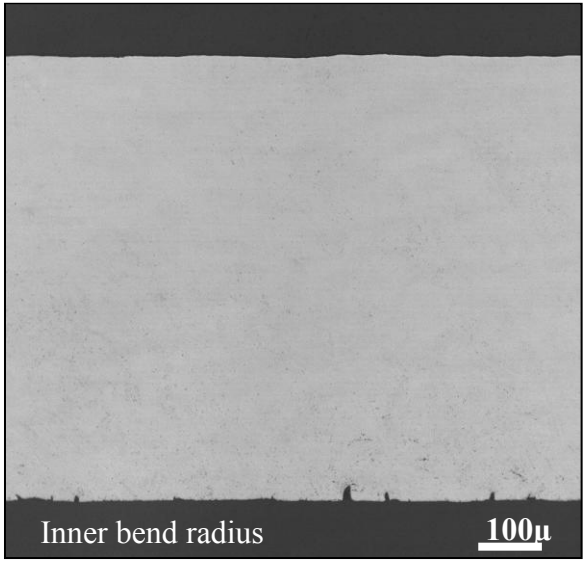

10 bend cycles

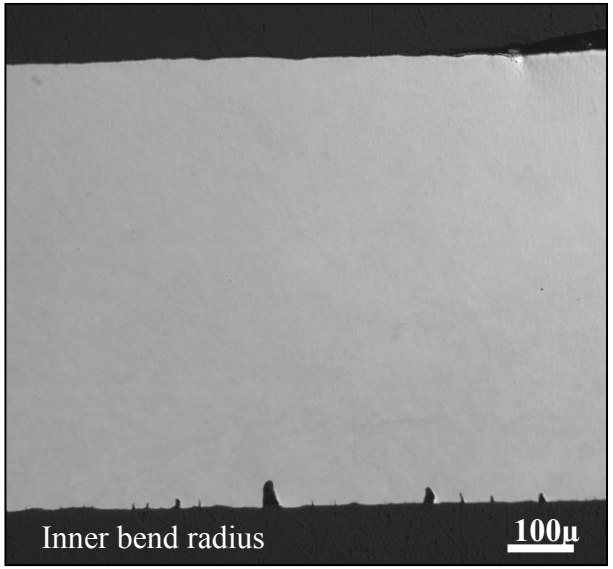

15 bend cycles

Figure 17 –
Photomicrographs of wall cross-sections depicting crack depths in differing # bend cycles.

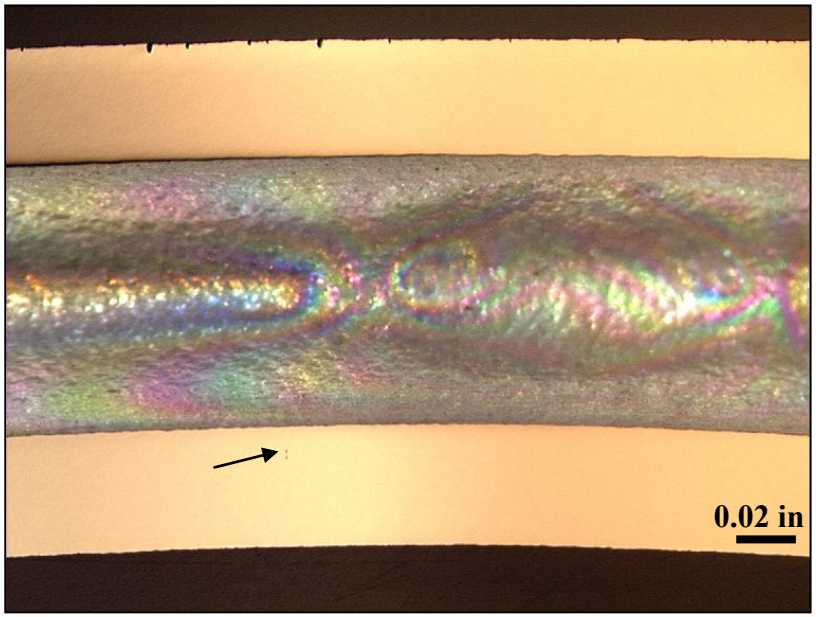

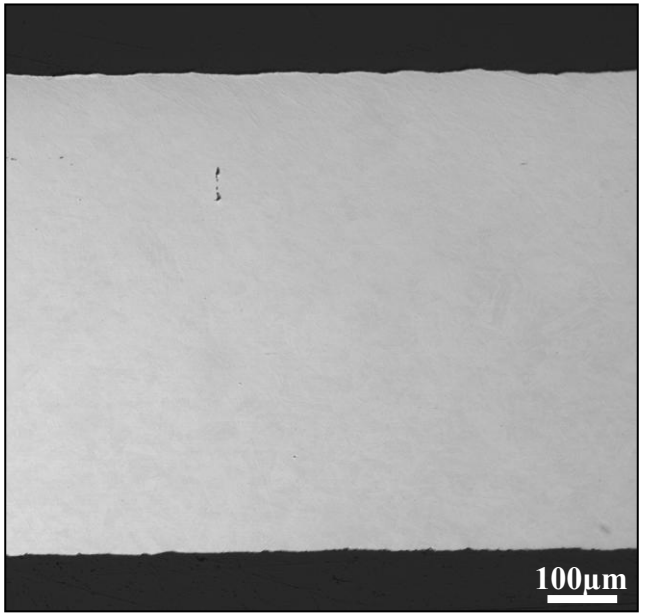

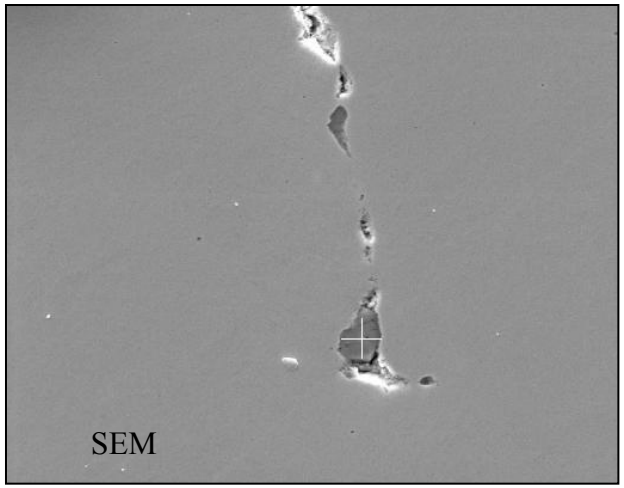

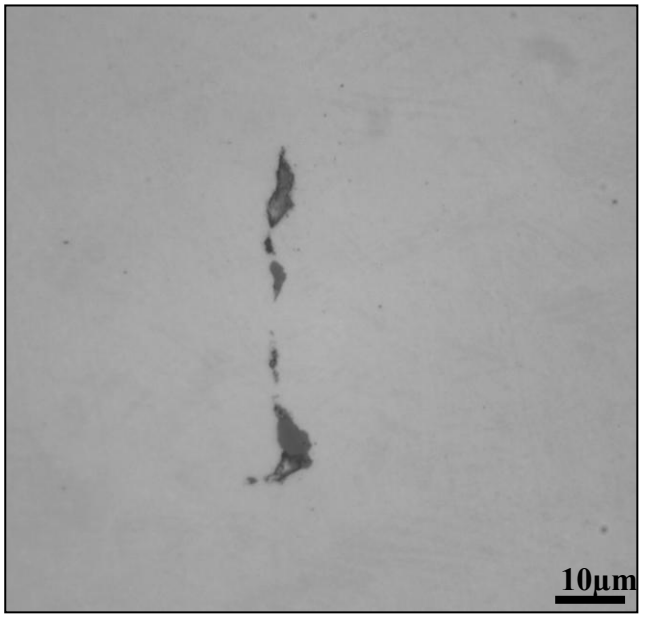

Figure 18 – Photomicrographs and SEM image of tube #11 (group 1 / 15 bends) cross-section exhibiting an inclusion. Chemical analysis revealed the primarily carbon and chromium constituents.